DEEP LEARNING FOR AN INVENTORY OF SMALL TO MIDSIZE VOLCANIC EDIFICES ON MARS.,
S. E. H. Sakimoto[1], D. D. Lewis[2], S. Dileep[3], P. Memon[3], J. R. Beveridge[3], N. T. Blanchard[3], T. K. P. Gregg[4], T. L. Carley[5] at [1]Space Science Institute, [2]David D. Lewis Consulting, [3]Colorado State Univ., Dept. of Computer Science, [4]Univ. at Buffalo, Dept. of Geology, [5]Lafayette College, Dept. of Geology and Environmental Geosciences.

Introduction: Volcanic constructs and their associated heat are critical to understanding both the geological evolution of Mars and its potential for past or current habitable environments. Although large (50-1500 km basal diameter) volcanic constructs are well documented, smaller volcanoes have been studied regionally (e.g. [1,2]). Datasets to support a global inventory are available, but are too vast for manual examination.

Machine learning is a potential solution [3]. Deep learning detectors have been demonstrated for impact craters [4], volcanic rootless cones transverse aeolian ridges [5], rockfalls [6], terrain types [7], and other landforms [8]. GPUs (graphics processing units) enable a planetary data set to be processed in days [9].

We demonstrate here that deep learning can easily detect small volcanic edifices in Martian data sets, and discuss its use in inventory construction.

Approach: We tested two techniques previously applied to crater detection: object detection with YOLO-v4 (You Only Look Once - v4) [10] and object segmentation using Mask R-CNN [9]. Mask R-CNN had higher accuracy in our test, so we report on it below.

The Mask R-CNN architecture proposes regions of interest, then generates bounding boxes and a semantic segmentation (pixel-level classification). We used a ResNet101 subnet for region proposal [11]. We tuned initial weights on the COCO (Common Objects in Context) data set [12].

Using JMARS Public 5.1.6 [13], we exported the MOLA (Mars Orbiter Laser Altimeter [14]) Colorized Elevation layer as JMARS JPEG gridded data at 128 pixels per degree (463 m/pixel at the equator) for 10 regional areas with small volcanoes in the Tempe Terra, Syria Planum, and Pavonis Mons SE areas [1, 2, 16-19].

MOLA images were randomly split into 7 training and 3 test (e.g. **Fig 1A**). Two novice annotators (computer science graduate students Dileep and Memon) outlined 230 readily apparent (steep) volcanic summits in training images. They did not attempt to identify more subtle edifices. Sakimoto, working separately from multiple data sets, mapped the apparent extent of all volcanic edifices in the test images, as well as tagging those with steep summits. Of 140 edifices in the test images, 45 had steep summits. Edifices ranged in size from 4 to ~80 km.

Contrast limited adaptive histogram equalization (CLAHE) was applied to all images. The 7 training images were increased to 63 by scaling, rotation, and flipping. MASK R-CNN parameters were fit on the 63 training images using stochastic gradient descent (SGD) and a minibatch size of 4 images.

The trained Mask R-CNN network was applied to the three test images at a detection probability threshold of 0.70. At this threshold, 43 of the 45 steep summits were uniquely detected in a single predicted bounding box (true positives). The remaining two were captured within the same bounding box. An additional 17 predicted bounding boxes contained no steep summit (false positives), 12 of which were volcanic constructs.

Replication with THEMIS Data. We conducted a second test with the same methods, but using THEMIS (Thermal Emission Imaging System [19]) daytime temperature data for 11 areas on the South and East lower flanks of Pavonis Mons volcano (JMARS exported JPEG gridded data at 256 pixels per degree, 231 m/pixel at the equator, e.g. **Fig. 1B**). For THEMIS data, the seven training images had 48 steep summits annotated. The four test images had 35 edifices mapped, of which 13 were tagged as having steep summits. At the 0.70 threshold, 12 of the 13 test steep summits were detected, with the single false negative cut off at the image's edge (**Fig. 1B**). There were 23 formal false positives, but one was a steep summit missed during test set annotation, 12 others were other volcanic constructs (shallow slope shields, lave tube ridges, rift vents, etc.).

Results: Figure 1 shows one MOLA and one THEMIS test image with the human-mapped edifices (colored polygons) and the Mask R-CNN bounding box predictions superimposed. Pink regions are volcanic edifices tagged as having a steep summit, and yellow are other volcanic edifices. Of the 16 steep summits in this MOLA image, all were detected. There were five false positives: one linear summit vent whose steep summit was separately detected, three volcanic edifices without steep summits, and one non-volcanic feature. For the THEMIS image, there were seven detections of steep summits, one false positive (a lava tube ridge), and the single false negative mentioned above.

Inventory Construction: Machine learning can aid, but not replace, geologist annotators. The morphological variety of volcanic edifices (particularly in polar regions), and the range of quantitative measurements and qualitative characterizations needed for a useful inventory, make manual mapping indispensable. Drawing on industrial annotation and work flow approaches, we are developing software for integrating annotation and machine learning in an active learning workflow [20].

Based on pilot studies and prior regional surveys, we expect 2000 or more volcanic edifices in the 3-50+

km range globally. We are training detectors for Context Camera (CTX) ([21]), Thermal Emission Imaging Spectrometer (THEMIS) daytime visible [22], THEMIS daytime IR, and MOLA data, as well as combinations of these. An accurate inventory with a minimum volcano size of 3 km basal diameter should be possible with 2000-3000 hours of geology student annotation effort, guided by machine learning and under planetary geologist supervision.

Conclusions: Although our pilot study targeted the most distinct edifices, the high accuracy achieved with minimal effort and training is encouraging. Our operational workflow will accumulate hundreds of times more training data, including informative examples chosen by active learning. MOLA data should support detecting shields with low flank slope, uniform visual appearance, irregular planform shape, and/or potential overlap with neighboring shields. Image data will likely excel for detecting visually distinctive edifices like rootless cones, shields with prominent radial flow textures, steep-sided cones, and embayed shields.

Acknowledgments: We used the THEMIS [22] and MOLA [23] PDS data for this work. https://planetarymaps.usgs.gov/mosaic/Mars_MO_THEMIS-IR-Day_mosaic_global_100m_v12.tif; https://doi.ord/10.1029/2000JE001364, https://planetarymaps.usgs.gov/mosaic/Mars_MGS_MOLA_DEM_mosaic_global_463m.tif

References: [1] Baptista et. al (2008) JGR, 113 (E9). [2] Bleacher, et. al (2009) JVGR, 185(1-2), 96-102. [3] Azari, et. al (2020), arXiv:2007.15129. [4] DeLatte, et. al (2019), Adv. Space Res., 64(8), 1615-1628.[5] Palafox, et. al (2017), Comp. & Geosci., 101, 48-56. [6] Bickel, et. al (2020), IEEE J. Sel. Topics Appl. Earth Obs. Remote Sens., 13, 2831-2841. [7] Balme, et. al (2019) LPSC (Vol. 50). [8] Wagstaff, et. al (2018) AAAI 2018. [9] Lee & Hogan (2020), arXiv:2010.12520. [10] Benedix, et al (2020), Earth and Space Science, 7(3), e01005. [11] He, et. al (2016), CVPR 2016, 770-778. [12] Lin, et. al (2014), Eur. Conf. Comp. Vision (740-755). Springer, Cham. [13] Christensen, et. al (2003), Science, 300(5628), 2056-2061. [14] Smith et al., 1992, JGR, 97(E5), pp771-7797. [16] Richardson, et. al (2013) JVGR, 252, 1-13. [17] Sakimoto, et. al (2003), Sixth Int. Conf. on Mars. [18] Baratoux, et. al (2011), Nature, 472(7343), 338-341. [19] Baratoux, et. al (2009), J Volcanology and Geothermal Research, 185(1-2), 47-68. [19] Christensen et al., 2004, Space Sci. Rev. 110 (1-2), pp85-130. [20] Settles, B. (2012). Active learning. Synthesis Lectures on Artificial Intelligence and Machine Learning, 6(1), pp.1-114. [21] Malin et al., (2007) JGR 112(E5). [22] Christensen, P.R., et al., (2004) *THEMIS Public Data Releases*, PDS Geosciences node, ASU, [23] Smith, D. E., et al. (2001). *JGR, 106*(E10), 23689–23722.

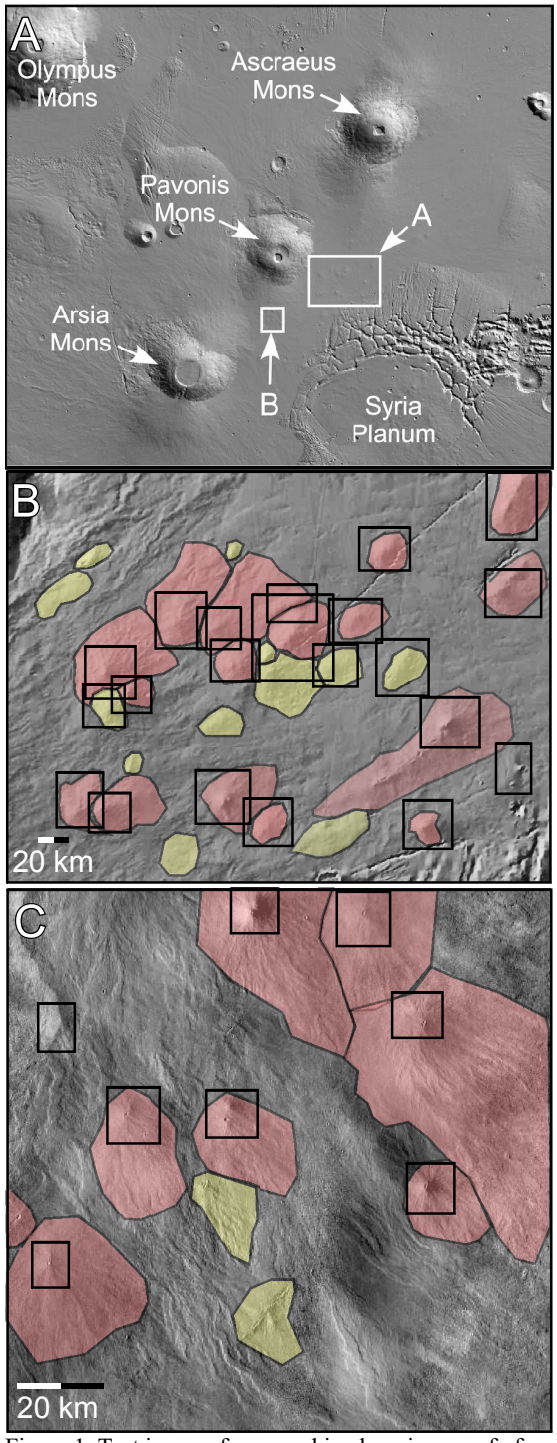

Figure 1. Test images from machine learning proof of concept study. A) MOLA regional topography showing the locations of figures (B) MOLA data centered at 1.603°S, 252.406° E. and (C THEMIS daytime infrared data centered at 4.867°S, 246.438°E.). Pink polygons indicate a steep summit volcanic edifice; all other volcanic edifices are yellow. The black boxes are machine learning edifice detections from a steep summit trained network.